Eur. Phys. J. B **20**, 397–403 (2001)

THE EUROPEAN PHYSICAL JOURNAL B

EDP Sciences

Escape of Brownian particles in a bistable sawtooth potential driven by correlated white noises

J.Y. You[1,2], L. Cao[1,2,3], S.Z. Ke[1,2,a], and D.J. Wu[2,3]

[1] State Key Laboratory for Laser Technology, Huazhong University of Science and Technology, Wuhan 430074, PR China
[2] Department of Physics, Huazhong University of Science and Technology, Wuhan 430074, PR China
[3] CCAST (World Laboratory), PO Box 8730, Beijing 100080, PR China

Received 16 September 2000 and Received in final form 15 January 2001

Abstract. An exact analytic expression of the relative escape rate (RER) for Brownian particles in a bistable sawtooth potential driven by correlated white noises is obtained. It is found that the RER *vs.* R (the multiplicative to the additive noise intensities ratio) exhibits a suppression platform for positive correlation, whereas the resonant activation and suppression platform appear successively for negative correlation. The mechanism of the present phenomena is explained. The effects of a nonlinear potential on the RER are studied. We have numerically calculated the RER of the system under a parabolic potential and a quartic potential and have compared the differences of the RER in the case of the linear potential and the one of the nonlinear potential.

PACS. 05.40.-a Fluctuation phenomena, random processes, noise, and Brownian motion – 82.40.Qt Complex chemical systems – 02.50.-r Probability theory, stochastic processes, and statistics

1 Introduction

The escape problem of Brownian particles has become ubiquitous in scientific fields, which has been widely studied in Markovian and non-Markovian processes since the pioneering contributions of Arrhenius and Kramers [1–3]. The early work mainly focused on the escape rate in a system driven by either additive or multiplicative noise. Doering and Gadoua investigated the activation rate of a system in the presence of a fluctuating barrier, they found a novel phenomenon called *Resonant Activation* [4]. Bier *et al.* studied the thermally driven escape rate over a dichotomously fluctuating barrier [5]. Furthermore, Madureira *et al.* considered a system driven simultaneously by uncorrelated multiplicative colored and additive white noises [6]. They discussed thermally driven escape from a double well over a fluctuating barrier in alternative approaches.

In recent years, the escape rate of a bistable system driven by correlated multiplicative and additive noises has attracted great interest. Madureira *et al.* have studied the escape rate of a bistable system driven by correlated additive and multiplicative white noises [7]. It is shown that the escape rate can exhibit *Giant Suppression* for a negative correlation coefficient between the additive and multiplicative noises. Fu *et al.* have studied the thermal activation problem of a bistable system driven by correlated multiplicative colored noise and additive white noise by means of numerical simulations [8]. The model describes the correlated function between noises as Dirac δ form. Moreover, Mei and Jia *et al.*, respectively, have examined the escape problem of a stochastic system with colored correlation between additive and multiplicative noises [9,10].

It must be pointed out that in a recent work by Tessone *et al.* [11], the idea of correlation between additive and multiplicative noises has been generalized to the study of stochastic resonance. In reference [11], the authors have analyzed the effects caused by the simultaneous presence of correlated additive and multiplicative noises on stochastic resonance. Besides the standard potential modulation, a time-periodic variation of the correlation between the two noise sources is also considered. It is seen that, stochastic resonance, characterized by the signal-to-noise ratio and the spectral amplification, is characteristically broadened. The broadening can be controlled by varying the relative phase shift between the two types of modulation force. And a remarkable aspect of the results indicates an alternative route of controlling the stochastic resonance phenomenon along the reasoning put forward in reference [12].

In reference [8], we have studied the escape rate of a bistable system driven by correlated multiplicative colored noise and additive white noise terms through numerical

[a] e-mail: szke@wuhan.cngb.com

simulations. However, the relevant analytical approach remains to further investigation. In order to see clearly the effects of the noise cross-correlation and "color" on the escape rate, the present paper, as a first stage, considers a piecewise linear potential model driven by correlated white noise terms. Based on the obtained exact analytical expression of the escape rate, one can further study the escape rate of particles in a piecewise linear potential with correlated colored and white noises. Moreover, it is possible to develop a general theory which is expected to extend the investigations of escape rates in generic systems driven by correlated colored and white noises. In the present paper, we consider two folds: One is to calculate the relative escape rate in a bistable sawtooth system which is driven by correlated multiplicative and additive white noises. The exact analytic expression of the relative escape rate is obtained. Some novel phenomena are presented. Another is to study the effects of a nonlinear potential of a system on the escape rate. The escape rates of the system driven by correlated multiplicative and additive white noises under a parabolic potential and a quartic potential are calculated, respectively. The differences of the escape rate in the case of the linear potential and the one of the nonlinear potential are compared. Also, the change of the escape rate with the increase of nonlinear degree of the potential is discussed.

2 General formula

We consider a one dimensional system driven by correlated multiplicative and additive noise, which is described by a Stratonovich Langevin equation,

$$\dot{x} = -V'(x) + g(x)\,\xi(t) + \eta(t), \tag{1}$$

where $V(x)$ is a potential function, and $\xi(t)$ and $\eta(t)$ are Gaussian white noises with

$$\begin{aligned} \langle \xi(t) \rangle &= \langle \eta(t) \rangle = 0, \\ \langle \xi(t)\,\xi(t') \rangle &= 2Q\delta(t-t'), \qquad (2) \\ \langle \eta(t)\,\eta(t') \rangle &= 2D\delta(t-t'), \qquad (3) \end{aligned}$$

and

$$\langle \xi(t)\,\eta(t') \rangle = \langle \xi(t')\,\eta(t) \rangle = 2\lambda\sqrt{QD}\,\delta(t-t'), \tag{4}$$

in which λ, the correlation coefficient, measures the degree of cross-correlation between the additive and multiplicative noises, Q is the strength of the multiplicative noise, and D the one of the additive noise.

Equation (1) together with equations (2–4) can be transformed into a equivalent stochastic differential equation [13]

$$\dot{x} = -V'(x) + G(x)\,\zeta(t), \tag{5}$$

where

$$\begin{aligned} G(x) &= D^{\frac{1}{2}}\left[Rg^2(x) + 2\lambda\sqrt{R}g(x) + 1\right]^{\frac{1}{2}}, \qquad (6) \\ \langle \zeta(t)\,\zeta(t') \rangle &= 2\delta(t-t'), \qquad (7) \end{aligned}$$

in which $R = Q/D$. The Fokker-Planck equation (FPE) corresponding to equation (5) with equations (6) and (7) is given by

$$\begin{aligned} \frac{\partial P(x,t)}{\partial t} = &-\frac{\partial}{\partial x}\left[-V'(x) + G(x)\,G(x')\right]P(x,t) \\ &+ \frac{\partial^2}{\partial x^2}G^2(x)\,P(x,t). \end{aligned} \tag{8}$$

The stationary probability density (SPD) can be obtained from equation (8)

$$P_{\rm st}(x) = \frac{N}{\left[Rg^2(x) + 2\lambda\sqrt{R}g(x) + 1\right]^{\frac{1}{2}}}\exp\left[-\Phi(x)/D\right], \tag{9}$$

where N is the normalization constant, and

$$\Phi(x) = \int^x V'(y)\,H^2(y)\,\mathrm{d}y, \tag{10}$$

$$H(x) = \left[Rg^2(x) + 2\lambda\sqrt{R}g(x) + 1\right]^{-\frac{1}{2}}. \tag{11}$$

When a particle passes through interval $[x_-, x_+]$ under a reflective and an absorbable boundary, the mean first passage time (MFPT) is determined by [1]

$$\begin{aligned} T_L(R,\lambda) = D^{-1}&\int_{x_-}^{x_+} H(x)\exp\left[\Phi(x)/D\right]\mathrm{d}x \\ &\times \int_{-\infty}^{x} H(y)\exp\left[-\Phi(y)/D\right]\mathrm{d}y. \end{aligned} \tag{12}$$

Here we define the escape rate κ as the inverse of the MFPT, *i.e.*, $\kappa = \frac{1}{T}$. For the convenience of discussion, we use the relative escape rate $\nu(R,\lambda)$ which is described by the following form

$$\nu(R,\lambda) = \frac{\kappa(R,\lambda)}{\kappa(R=0)} = \frac{T(R=0)}{T(R,\lambda)}\cdot \tag{13}$$

3 Linear model

The potential of the bistable sawtooth model is assumed as

$$V(x) = \begin{cases} -2bx/L - 2b, & -\infty < x \le -L/2 \\ 2bx/L, & -L/2 \le x \le 0 \\ -2bx/L, & 0 \le x \le L/2 \\ 2bx/L - 2b, & L/2 \le x < \infty \end{cases}, \tag{14}$$

and $g(x)$ is given by

$$g(x) = \begin{cases} c, & -\infty < x \le -L/2, \quad 0 < x \le L/2 \\ -c, & -L/2 < x \le 0, \quad L/2 < x < \infty \end{cases}. \tag{15}$$

$$H(x)=\begin{cases}\alpha^{-\frac{1}{2}}=\left[c^2R+2\lambda c\sqrt{R}+1\right]^{-\frac{1}{2}}, & -\infty<x\le -L/2, \quad 0<x\le L/2\\ \beta^{-\frac{1}{2}}=\left[c^2R-2\lambda c\sqrt{R}+1\right]^{-\frac{1}{2}}, & -L/2<x\le 0, \quad L/2<x<\infty\end{cases},$$

Now we derive the MFPT when a particle goes through the interval $[-L/2, L/2]$. Combining equation (12) with equations (14–15), the MFPT is obtained

$$T_{\mathrm{L}}(R,\lambda)=D^{-1}\int_{-L/2}^{L/2}H(x)\exp\left[\Phi(x)/D\right]\mathrm{d}x \times\int_{-\infty}^{x}H(y)\exp\left[-\Phi(y)/D\right]\mathrm{d}y, \quad (16)$$

where

See equation above

and $\Phi(x)$ is given by equation (10).

The exact analytical expression of equation (16) can be derived by means of partial integration,

$$\begin{aligned}T_{\mathrm{L}}(R,\lambda)=\frac{L^2D}{4b^2}\Big[&(\alpha\beta)^{\frac{1}{2}}\left[\exp(q/\alpha)\left(1-\exp(-q/\beta)\right)\right.\\&+\left(1-\exp(q/\beta)\right)\left(\exp(-q/\alpha)-1\right)]\\&+\alpha\left[\exp(q/\alpha)+\exp(-q/\alpha)-2\right]\\&+\beta\left[\exp(q/\beta)-1\right]\Big],\end{aligned} \quad (17)$$

where $q=b/D$. For $R=0$, the case without multiplicative noise, one obtains

$$T_{\mathrm{L}}(R=0)=\frac{L^2D}{4b^2}\left[4\exp(q)+2\exp(-q)-6\right]. \quad (18)$$

and for $\lambda=0$, the case of independent noises, the MFPT becomes

$$T_{\mathrm{L}}(\lambda=0)=\frac{L^2D}{4b^2}\left[4\exp\left(\frac{q}{c^2R+1}\right)+2\exp\left(-\frac{q}{c^2R+1}\right)-6\right]\left(c^2R+1\right). \quad (19)$$

Inserting equations (17, 18) into equation (13), we finally obtain the relative escape rate when particles pass through interval $\left[-\frac{L}{2},\frac{L}{2}\right]$,

$$\nu_{\mathrm{L}}(R,\lambda)=\frac{T_{\mathrm{L}}(R=0)}{T_{\mathrm{L}}(R,\lambda)}=\frac{4\exp(q)+2\exp(-q)-6}{W_{\mathrm{L}}(R,\lambda)}, \quad (20)$$

where

$$\begin{aligned}W_{\mathrm{L}}(R,\lambda)=&(\alpha\beta)^{\frac{1}{2}}\left[\exp(q/\alpha)\left(1-\exp(-q/\beta)\right)\right.\\&+\left(1-\exp(q/\beta)\right)\left(\exp(-q/\alpha)-1\right)]\\&+\alpha\left[\exp(q/\alpha)+\exp(-q/\alpha)-2\right]\\&+\beta\left[\exp(q/\beta)-1\right].\end{aligned}$$

In particular, for $\lambda=0$, we have

$$\nu_{\mathrm{L}}(\lambda=0)=\frac{(2\exp(q)+\exp(-q)-3)}{\left[2\exp\left(\frac{q}{c^2R+1}\right)+\exp\left(-\frac{q}{c^2R+1}\right)-3\right](c^2R+1)}. \quad (21)$$

4 Nonlinear model

In the following, we discuss the relative escape rate of Brownian particles under two kinds of nonlinear bistable potentials with the same coefficient of the multiplicative noise. The effects of the potential nonlinearity on the relative escape rate are analyzed by means of numerical calculations. First, the relative escape rate of the particles which goes through the parabolic potential is calculated, then the case of the quartic potential is considered.

We assume the coefficient of the multiplicative noise has the following form

$$g(x)=\begin{cases}c, & -\infty<x\le -1, \quad 0<x\le 1\\ -c, & -1<x\le 0, \quad 1<x<\infty\end{cases}. \quad (22)$$

4.1 Parabolic bistable potential

The nonlinear parabolic bistable potential is considered as a second order approximation of a quartic potential (*i.e.*, $-x^2/2+x^4/4$) [14]

$$V(x)=\begin{cases}\frac{1}{4}\left[\frac{\sqrt{3}}{\sqrt{3}-1}(x+1)^2-1\right], & x\le -\frac{1}{\sqrt{3}}\\ -\frac{1}{4}\left[\sqrt{3}x^2\right], & -\frac{1}{\sqrt{3}}\le x\le\frac{1}{\sqrt{3}}\\ \frac{1}{4}\left[\frac{\sqrt{3}}{\sqrt{3}-1}(x-1)^2-1\right], & x\ge\frac{1}{\sqrt{3}}\end{cases}. \quad (23)$$

Inserting equations (22, 23) into equation (12), we obtain MFPT of particles pass through interval $[-1, 1]$

$$T_{\mathrm{P}}(R,\lambda)=D^{-1}\int_{-1}^{1}H(x)\exp\left[\Phi(x)/D\right]\mathrm{d}x \times\int_{-\infty}^{x}H(y)\exp\left[\Phi(y)/D\right]\mathrm{d}y, \quad (24)$$

$$H(x)=\begin{cases}\alpha^{-\frac{1}{2}}=\left[c^2R+2c\lambda\sqrt{R}+1\right]^{-\frac{1}{2}}, & -\infty<x\leq -1, \quad 0<x\leq 1\\ \beta^{-\frac{1}{2}}=\left[c^2R-2c\lambda\sqrt{R}+1\right]^{-\frac{1}{2}}, & -1<x\leq 0, \quad 1<x<\infty\end{cases}. \tag{25}$$

$$H(x)=\begin{cases}\alpha^{-\frac{1}{2}}=\left[c^2R+2c\lambda\sqrt{R}+1\right]^{-\frac{1}{2}}, & -\infty<x\leq -1, \quad 0<x\leq 1\\ \beta^{-\frac{1}{2}}=\left[c^2R-2c\lambda\sqrt{R}+1\right]^{-\frac{1}{2}}, & -1<x\leq 0, \quad 1<x<\infty\end{cases}. \tag{29}$$

where

See equation (25) above.

Since equation (24) can not be integrated exactly, we work out $T_{\mathrm{P}}(R,\lambda)$ by means of numerical integration, and then calculate the relative escape rate

$$\nu_{\mathrm{P}}(R,\lambda)=\frac{T_{\mathrm{P}}(R=0)}{T_{\mathrm{P}}(R,\lambda)}. \tag{26}$$

4.2 Quartic bistable potential

The quartic potential are defined as

$$V(x)=-\frac{1}{2}x^2+\frac{1}{4}x^4. \tag{27}$$

The MFPT of particles pass through the interval $[-1,1]$ reads

$$T_{\mathrm{Q}}(R,\lambda)=D^{-1}\int_{-1}^{1}H(x)\exp\left[\Phi(x)/D\right]\mathrm{d}x \times\int_{-\infty}^{x}H(y)\exp\left[\Phi(y)/D\right]\mathrm{d}y, \tag{28}$$

where

See equation (29) above.

Also, equation (29) can not be integrated precisely, we calculate $T_{\mathrm{Q}}(R,\lambda)$ by numerical integration, and get the relative escape rate

$$\nu_{\mathrm{Q}}(R,\lambda)=\frac{T_{\mathrm{Q}}(R=0)}{T_{\mathrm{Q}}(R,\lambda)}. \tag{30}$$

5 Conclusions and discussions

5.1 The relative escape rate in a linear potential field

From equation (20), we can see that the relative escape rate $\nu_{\mathrm{L}}(R,\lambda)$ in the linear potential field is not affected by the width of the linear potential L since the expression $\nu_{\mathrm{L}}(R,\lambda)$ is independent of L. However, the relative escape rate is very sensitive to the parameter q ($q=b/D$) and the coefficient of multiplicative noise c. When R is large enough ($R\gg 1$), $W(R,\lambda)$, the denominator of equation (20), approaches to $2q$, thus the relative escape rate ν_{L} tends to be a constant for a fixed value q. The curves of $\nu_{\mathrm{L}}\sim R$ can exhibit different structures for different values of λ.

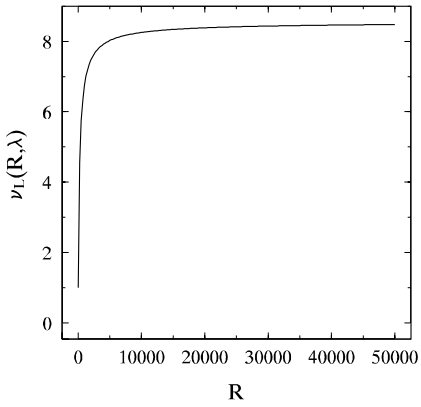

Fig. 1. Relative escape rate $\nu_{\mathrm{L}}(R,\lambda)$ *vs.* R at $b=0.25$, $c=0.125$, $D=0.1$, and $\lambda=0.2$.

(a) For small positive values of λ (*e.g.*, $\lambda=0.2$), ν_{L} increases sharply with the increasing of R at first, then the increase of ν_{L} becomes slow, and finally ν_{L} approaches to a fixed value when R is increased large enough, as shown in Figure 1. In this case, there is no extremum. However, for $\lambda\geq 0.4$, a *suppression platform* appears in the curve of $\nu_{\mathrm{L}}-R$ when R is relatively small, and the suppression platform becomes wider as λ increases, which are presented in Figure 2a. Also, when R is large enough, ν_{L} tends to a fixed value, as shown in Figure 2b.

(b) Figures 3a, b show that, for $\lambda<0$, ν_{L} exhibits one-minimum and one-maximum structure. When R increases at the beginning, the suppression platform appears; and it becomes wider as λ decreases; as R increases continuously, a peak emerges, which is called *resonant activation*, and the peak grows higher as λ decreases. When R is large enough, ν_{L} gradually decreases to a fixed value.

From the points of view of mathematics and physics, the mechanism of the presented phenomena can be understood as follows. For $\lambda<0$, $\alpha=c^2R+2c\lambda\sqrt{R}+1$, and

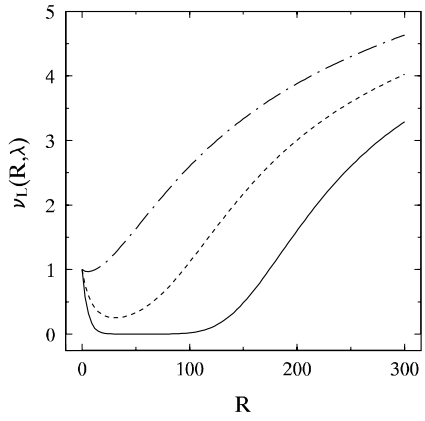

(a)

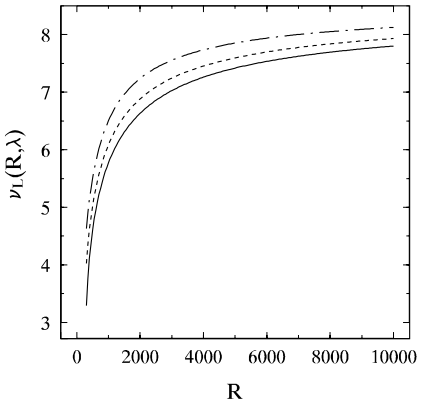

(b)

Fig. 2. Relative escape rate $\nu_{\mathrm{L}}(R,\lambda)$ *vs.* R at $b = 0.25$, $c = 0.125$ and $D = 0.1$ for different values of the correlation coefficient: $\lambda = 0.9$ (solid line), $\lambda = 0.7$ (dashed line), and $\lambda = 0.4$ (dash-dotted line). R varies in (a) $R \in [0, 300]$; (b) $R \in [300, 10\,000]$.

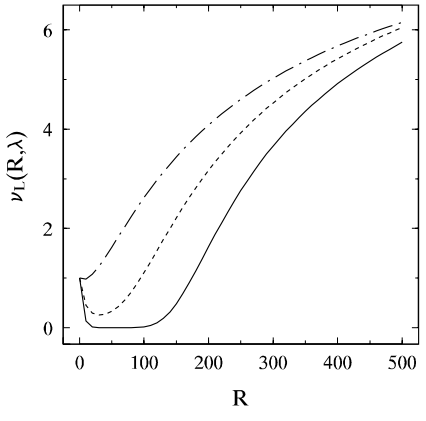

(a)

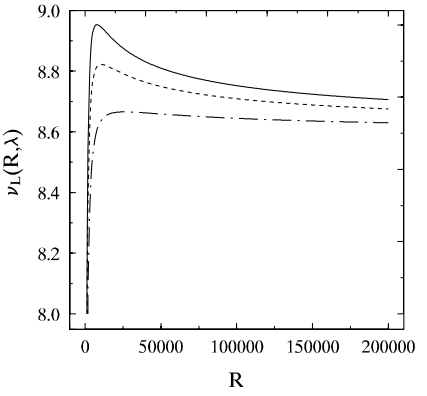

(b)

Fig. 3. Relative escape rate $\nu_{\mathrm{L}}(R,\lambda)$ *vs.* R at $b = 0.25$, $c = 0.125$, and $D = 0.1$ for different values of the correlation coefficient: $\lambda = -0.9$ (solid line), $\lambda = -0.7$ (dashed line), and $\lambda = -0.4$ (dash-dotted line). R varies in (a) $R \in [0, 500]$; (b) $R \in [500, 200\,000]$.

for $\lambda > 0$, $\beta = c^2R - 2c\lambda\sqrt{R} + 1$, both α and β have a minimum at $R_{\mathrm{m}} = \lambda^2/c^2$. Particularly, in the case of perfectly positive correlation $\lambda = 1$, $\alpha = \left(c\sqrt{R} - 1\right)^2$; also $\beta = \left(c\sqrt{R} - 1\right)^2$ in the case of perfectly negative correlation $\lambda = -1$. These cases lead to $R_{\mathrm{m}} = 1/c^2$, α and β vanish, $\mathrm{e}^{q/\alpha}$ and $\mathrm{e}^{q/\beta}$ approach to infinity, and $W(R,\lambda)$ in equation (20) tends to infinity. Consequently, the relative escape rate ν_{L} approaches to zero. Even R varies near R_{m}, $W(R,\lambda)$ is large enough, and ν_{L} is still small. so that suppression platform appears in Figures 2a and 3a. Indeed, $\alpha = 0$ or $\beta = 0$ implies that the effective noises disappear, so that particles are in deterministic potential field and can not surmount the barrier. On the other hand, for $\lambda < 0$, the $W(R,\lambda) \sim R$ curve exists the two extrema according to the extremal equation of $W(R,\lambda)$ in equation (20), but has only one extremum for $\lambda > 0$. Therefore, resonant activation and suppression platform appear successively in the case of $\lambda < 0$, as shown in Figure 3, and there only exists the suppression platform in the case of $\lambda > 0$. In fact, in the case of $\lambda < 0$, the effective noise intensity in equation (15) is taken as $\beta = c^2R + 1 + 2|\lambda| c\sqrt{R}$, in comparison with that of $\lambda > 0$, the effective noise intensity in equation (15) taken as $\alpha = c^2R + 1 - 2\lambda c\sqrt{R}$, one has $\beta > c^2R + 1 > \alpha$, which means particles pass through the barrier more easily for $\lambda < 0$ than the one for $\lambda > 0$, thus leads to rather different tendencies between $\nu_{\mathrm{L}}(\lambda > 0)$ and $\nu_{\mathrm{L}}(\lambda < 0)$ for $R \to \infty$ in equation (20). $\nu_{\mathrm{L}}(R, \lambda < 0)$ is down to $\nu_{\mathrm{L}}(R = \infty, \lambda)$, whereas $\nu_{\mathrm{L}}(R, \lambda > 0)$ is up to $\nu_{\mathrm{L}}(R = \infty, \lambda)$, so that $\nu_{\mathrm{L}}(R, \lambda < 0)$ is bound to experience the process from the suppression platform to the resonant activation as R increases continuously.

5.2 The comparison of the relative escape rate in different potential fields

Equations (26) and (30) are calculated numerically, and the relative escape rate as a function of R in the parabolic

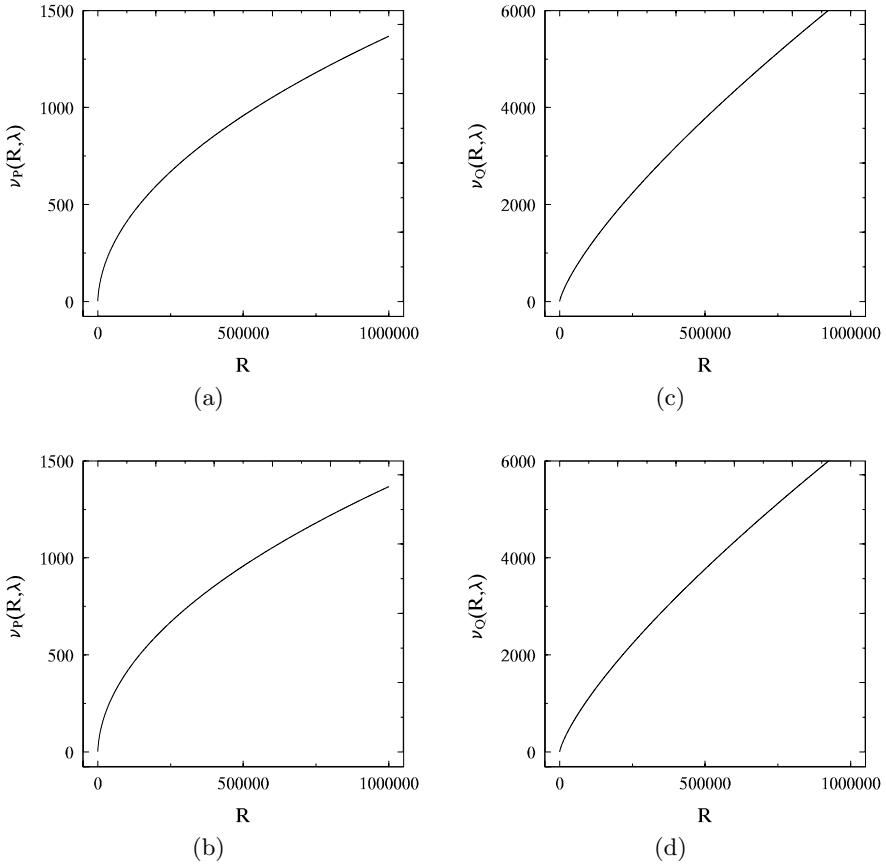

Fig. 4. (a) Relative escape rate $\nu_{\rm P}(R,\lambda)$ *vs.* R in the parabolic potential at $\lambda = 0.2$; (b) Relative escape rate $\nu_{\rm P}(R,\lambda)$ *vs.* R in the parabolic potential at $\lambda = -0.2$; (c) Relative escape rate $\nu_{\rm Q}(R,\lambda)$ *vs.* R in the quarlic potential at $\lambda = 0.2$; (d) Relative escape rate $\nu_{\rm Q}(R,\lambda)$ *vs.* R in the quarlic potential at $\lambda = -0.2$. The other parameters are $c = 0.125$ and $D = 0.1$.

and quarlic potential fields is drawn in Figures 4–6, respectively.

Figures 4a–d show that, when the value of the correlation coefficient is small, the relative escape rate is always increased monotonously with the increasing of R whatever the nonlinear potential field is parabolic or quarlic, or the correlation coefficient is positive or negative, which are different from that in the linear potential field for $R \gg 1$. Meanwhile, in Figures 5 and 6, when $|\lambda|$ is large, the relative escape rate only exhibits the suppression platform. From this point of view, the resonant activation disappears due to the nonlinearity of the potential field.

The effects of the nonlinear degree of the potential field on the relative escape rate are shown in Figures 5 and 6. When D is small and $\lambda < 0$, the relative escape rate in the parabolic potential is close to that in the quartic potential (see Fig. 5). However, Figures 6a, b show that, when D is large, the relative escape rate in quartic potential is always less than the case in the parabolic potential for $\lambda < 0$. By contraries, the relative escape rate in quartic potential is always larger than the case in the parabolic potential for $\lambda > 0$.

In conclusion, we make a discussion of the results in relation with some concrete applications. As indicated in

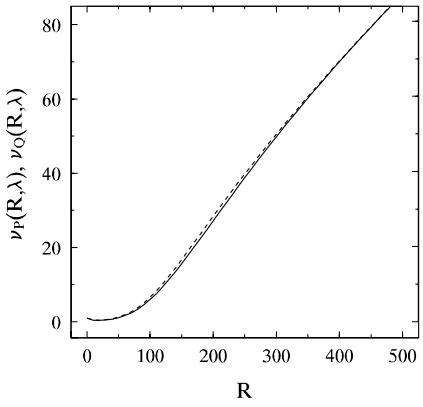

Fig. 5. Comparison of relative escape rate $\nu_{\rm P}(R,\lambda)$ *vs.* R to relative escape rate $\nu_{\rm Q}(R,\lambda)$ *vs.* R at $c = 0.125$, $D = 0.05$, and $\lambda = -0.5$. $\nu_{\rm P}(R,\lambda)$ is indicated by the dashed line, and $\nu_{\rm Q}(R,\lambda)$ is indicated by the solid line.

reference [7], there exist realistic models showing bistability, where the fluctuations in the model parameters are not independent and such fluctuations do lead to noise contributions of both additive and multiplicative character. The potential physical application is given by the switching

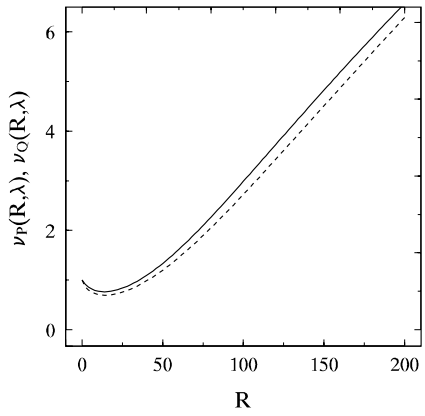

Fig. 6. Comparison of relative escape rate $\nu_{\rm P}(R,\lambda)$ *vs.* R to relative escape rate $\nu_{\rm Q}(R,\lambda)$ *vs.* R at $c = 0.125$ and $D = 0.1$ for (a) $\lambda = 0.5$, and (b) $\lambda = -0.5$. $\nu_{\rm P}(R,\lambda)$ is indicated by the dashed line, and $\nu_{\rm Q}(R,\lambda)$ is indicated by the solid line.

of magnetization in single-domain ferromagnetic particles in which external and internal magnetic field fluctuations are generally correlated and mutually influence the bistable relaxation dynamics of the magnetic moment. Moreover, the phenomena of resonant activation and suppression platform and their variation are revealed in the present work, which may crucially affect the transport in the bistable system and indicate an alternative route of controlling the escape phenomenon by varying the correlation coefficient and the intensity ratio of the two noises. Therefore, one can follow the procedure in reference [11] to physically realize the controlling of correlation coefficient and intensity ratio of the two noises by means of an electronic circuit with two different white noise sources.

This work has been supported by the National Natural Science Foundation of China under grant No. 19975020.

References

1. P. Hänggi, P. Talkner, M. Borkovec, Rev. Mod. Phys **62**, 251 (1990).
2. V.I. Mel'nikov, S.V. Meshkov, J. Chem. Phys. **85**, 1018 (1986).
3. A.N. Drozdov, Phys. Rev. E **58**, 2865 (1998).
4. C.R. Doering, J.C. Gadoua, Phys. Rev. Lett. **69**, 2318 (1992).
5. M. Bier, R.D. Astuonian, Phys. Rev. Lett. **71**, 1649 (1993).
6. A.J.R. Madureira, P. Hänggi, V. Buonomano, W.A. Rodrigues Jr, Phys. Rev. E **51**, 3849 (1995).
7. A.J.R. Madureira, P. Hänggi, H.S. Wio, Phys. Lett. A **271**, 248 (1996).
8. Fu Hai-Xiang, Cao Li, Wu Da-Jin, Phys. Rev. E **59**, R6235 (1999).
9. Mei Dong-Cheng, Xie Guang-Zhong, Cao Li, Wu Da-Jin, Phys. Rev. E **59**, 3880 (1999).
10. Y. Jia, J.R. Li, Physica A **252**, 417 (1998).
11. C.J. Tessone, H.S. Wio, P. Hänggi, Phys. Rev. E **62**, 4623 (2000); C.J. Tessone, H.S. Wio, Mod. Phys. Lett. B **12**, 1195 (1998).
12. L. Gammaitoni, M. Löcher, A. Bulsara, P. Hänggi, J. Neff, K. Wiesenfeld, W. Ditto, M.E. Inchiosa, Phys. Rev. Lett. **82**, 4574 (1999).
13. Wu Da-Jin, Cao Li, Ke Sheng-Zhi, Phys. Rev. E **50**, 2496 (1994).
14. F. Castro, H.S. Wio, G. Abramson, Phys. Rev. E **52**, 159 (1995).